Influence of hydrodynamics on the water pathway and spatial distribution of pesticide and metabolite concentrations in constructed wetlands

Celine Gaullier, Sylvie Dousset, Nicole Baran, Geraldine Kitzinger, Charlotte Coureau

Influence of hydrodynamics on the water pathway and spatial distribution of pesticide and metabolite concentrations in constructed wetlands

Céline Gaullier [(1, 2, 3)], Sylvie Dousset [(1, 3)*], Nicole Baran [(2)], Géraldine Kitzinger [(1)], Charlotte Coureau[(2)]

[(1)] *Laboratoire Interdisciplinaire des Environnements Continentaux, Université de Lorraine - CNRS, 54506 Vandœuvre-lès-Nancy*

[(2)] *BRGM, 45060 Orléans CEDEX 02, France*

[(3)]*LTSER France, Zone Atelier du Bassin de la Moselle, 54506 Vandœuvre-lès-Nancy, France*

*Corresponding author

sylvie.dousset@univ-lorraine.fr

Sylvie DOUSSET

Laboratoire Interdisciplinaire des Environnements Continentaux

Université de Lorraine - CNRS,

BP 70239 - Bd des Aiguillettes

54506 Vandœuvre-lès-Nancy

Tel.: +33 (0)3 72 74 52 12

Nomenclature

σ_θ^2	RTD variance
θ	dimensionless time
λ	hydraulic efficiency
e_v	effective volume ratio
HRT	hydraulic residence time
N	number of serial mixing tanks
Pe	Peclet number
RTD	residence time distribution
t_n	theoretical residence time
t_{mean}	mean residence time
t_{10}/t_n	time to recover 10 % of the injected tracer
t_{90}/t_n	time to recover 90 % of the injected tracer
t_{90}/t_{10}	Morrill index

Abstract

Constructed wetlands (CWs) are likely to reduce pesticide levels reaching surface water. However, the distribution of the water flow path between the main channel and isolated areas may influence global pesticide mitigation. Little information is known about the influence of water pathways on pesticide mitigation. Thus, we performed tracer experiments at low and high flow rates (0.5 L/s and 4-7 L/s) in a pond CW and ditch CW to determine the localization of various hydraulic zones and to understand their implication on pesticide mitigation. The hydraulic performance reflecting the fraction of water transported from inlet to outlet passing through the whole of CW, was greater for the pond CW than for the ditch CW regardless of the flow rate, and greater at mean flow rates (MF) than at low flow rates (LF) due to a lower proportion of isolated areas at a MF (11 % - 68 %) than at LF (38 % - 89 %). Dispersion governed the water transport inside the isolated areas and the water convection inside the main channel. Consequently, dissolved pesticide concentrations are heterogeneously distributed in the CWs, i.e., in the main channel and isolated area, for both flow rates. However, one month after a no-flow period, this heterogeneity disappears, and dissolved pesticide concentrations become similar in the water of the whole CW due to dispersion. Furthermore, sedimentation and storage in sediments were greater in the isolated area than in the main channel, which is possibly due to a lower speed flow rate and a higher hydraulic residence time (HRT) in the isolated area than in the main channel. Thus, isolated areas act as effective's zones to mitigate pesticides from dissolved and particulate phases inside the CW during a complete drainage season (i.e., succession of high/low/no-flow periods).

Keywords:

Pond, ditch, isolated area, main channel, convection, dispersion

1. Introduction

To protect or restore the surface water quality as required by the EU Water Framework Directive (JOCE, 2000), constructed wetlands (CWs) have been presented as a potential solution for reducing agricultural inputs such as nitrates and pesticides in surface water (Alvord and Kadlec 1996; Gregoire et al. 2009; Vymazal and Březinová 2015). These CWs have emerged as a cost-effective practice to reduce contaminant loading from drainage (Schultz et al. 1995; Moore et al. 2001; Tournebize et al. 2012; Vallée et al. 2015) and have been described as good environmental practices (JOCE, 2006). A recent review summarizes 32 studies related to the remediation of organophosphorus pesticides in 117 CWs during 2001–2017 worldwide, shown that organophosphorus pesticides were removed with efficiency up to 87 ± 16.6% (Liu et al. 2019). Another study reported efficiency removal > 80 % for 8 pesticides in a CW with a HRT varying from 3 to 35 days (Maillard and Imfeld 2014). On the contrary, another study reported efficiency removal varying from -50% to 14% in mean for 15 pesticides in 2 CWs, with a HRT varying from 5 h to 17 days (Vallée et al. 2015b). These authors have suggested that major processes are pesticide adsorption and degradation. The main processes of dissolved pesticide mitigation from CW water are adsorption on sediments (Matamoros et al. 2008; Stehle et al. 2011), absorption by plants (Moore et al. 2013) and degradation in aqueous or sediment phases (Elsayed et al. 2014). The main process of particulate pesticide removal is the sedimentation of total suspended solids (TSS) on which pesticides are adsorbed (Koskiaho 2003; Maillard et al. 2011).

Some studies reported the important role of hydraulic parameters on pesticide mitigation. For example, the hydraulic residence time (HRT), which indicates how long the inflow is retained in the wetland, is considered to be one of the main factors influencing the pesticide mitigation effectiveness of CWs (Elsaesser et al. 2011; Stehle et al. 2011; Vallée et

al. 2015). Generally, the mean HRT, determined with tracer data, is shorter than the nominal HRT (corresponding to the ratio of wetland volume on the flow rate) due to the presence of short-circuits, inducing a decrease in the hydraulic performance; i.e., the total CW volume is not affected by water (Martinez and Wise 2003). Short-circuits have been reported as one of the main drawbacks to the effectiveness of CWs because water is transported from the inlet to the outlet by preferential flow, which decreases the mean HRT and the effective volume (i.e., the CW volume used for pesticide mitigation) (Thackston et al. 1987). Schematically, the volume of the CW can be divided into three hydraulic zones (Kadlec 1994; Werner and Kadlec 2000; Martinez and Wise 2003): (1) a main channel with preferential flow; (2) a temporary storage zone (mixing zone) showing exchanges with the main channel; and (3) a dead zone, which is more isolated from the main channel than the mixing zone. The mixing and dead zones are considered isolated areas (Martinez and Wise 2003) and are differentiated by their exchange rate with the main channel, such as a lower water speed and solute dispersion in the case of dead zones than in mixing zones. The distribution of these three hydraulic zones could be spatially and temporally influenced by (i) CW morphology: the length-to-width ratio, the inlet/outlet configurations and the presence of obstructions (Su et al. 2009), and by (ii) hydraulic parameters such as HRT, flow rate and water depth (Liu et al. 2016; Shih et al. 2017).

Thus, considering that at a local scale inside the CW, the HRT occurring in the isolated areas could be longer than in the main channel, we can hypothesize that pesticide mitigation processes such as adsorption, absorption, and degradation would be enhanced in these areas. In addition, these hydraulic zones might move inside the CW depending of the flow rate changes in the field. To our knowledge, there is no study regarding the role of these hydraulic zones such as the main channel and isolated zones on pesticide and metabolite mitigation.

Thereby, we investigated the influence of the flow rate on the water pathway distribution (main channel, isolated areas) in two CWs (a succession of three ponds and a ditch with lateral enlargement) and subsequently on the mitigation of pesticides and metabolites in dissolved and particulate phases. Bromide-tracing experiments were carried out at 3 flow rates in the pond and at 2 flow rates in the ditch. In addition, the spatial distribution of pesticide and metabolite concentrations in aqueous (dissolved and particulate) and sediment phases was evaluated to determine the contribution of the main channel and isolated areas to pesticide and metabolite mitigation.

2. Materials and methods

2.1. Constructed wetlands

The two CWs are located under temperate climate, with mean precipitation varying from 1.9 to 3.5 mm/day and mean water volume drained varied from 0.3 to 4.5 mm/day. The dominant cultures on crop fields are wheat, barley, maize and rapeseed (Table 1). More details about climatological, hydraulic and agricultural context of these two CWs are given in Table 1.

The two studied CWs were built in autumn 2010 in a regulatory grass strip, and spontaneous vegetation recovered the entire CW in two years. Thus, during our experiments, the vegetation was present throughout the year, and its influence on the hydrodynamic dispersion as reported by Jenkins and Greenway (2005) could be considered similar under all seasons. The first CW located at Ville-sur-Illon (75 km at the South of Nancy, France) consisted roughly of a succession of three ponds of 47.8 m length and 4 to 6.5 m width, with a surface of 215 m^2 and an island at the beginning of the second pond (Fig. 1). It received the drainage water from an 8 ha plot (cambisol, FAO 2006) by a drain collector located at inlet of

142 the CW. The CW was entirely vegetated and dominated by *Juncus effusus, Juncus inflexus,*
143 and *Juncus articulatus* on the edge of the CW, with *Typha latifolia, Typha angustifolia*,
144 *Epilobium hirsutum* and *Veronica becabunga* inside the CW. The second CW located at
145 Manoncourt-sur-Seille (30 km in the North of Nancy, France) consisted roughly of a ditch of
146 80 m length and 0.9 m width, and it expanded over 12 m long by 4 m wide, with a surface of
147 100 m^2 (Fig. 1). It received the drainage water from a 10 ha plot (gleyic cambisol, FAO
148 2006). The CW was entirely vegetated and dominated by *Juncus effusus, Juncus*
149 *conglomerates* and grasses. Substrates of both CWs were clayed, which allowed their
150 imperviousness. Both CWs have been precisely topographically levelled allowing the
151 determination of water volume.
152
153 *2.2. Tracer experiment*
154
155 The inlet and outlet flow rates were measured continuously using a pollubac (1515 DA,
156 POLLUBAC®) and an ultra-sound flow meter (950-US 50 Hz, SIGMA); a mean flow rate
157 was recorded every 30 min of measurement. Three experiments were conducted in the pond
158 CW (at high flow = HF, mean flow = MF and low flow = LF), and two were conducted in the
159 ditch CW (MF and LF) (Table 2). All tracer tests were conducted in dry weather conditions,
160 so no precipitation must be considered. However, despite no rainfall, flow rates varied
161 between the beginning and the end of the tracer experiments. Of the five tracer experiments,
162 flow rates varied from 3 % (pond-HF) to 30 % (pond-LF) (Table 2). The estimation of the
163 water transport parameters was done considering a constant flow rate, which was chosen as
164 the mean flow rate (Table 2). The CW's water volume was monitored manually thanks to
165 limnimetric scales (one limnimetric scale is localised in each of the 3 pond and in each of the
166 3 parts of the ditch). Besides, CW's geometries were determined by topographic

167 measurements. For each tracer experiment, the volume of water was calculated with
168 Autocad® and ADTOPO® softwares based on water level observed in the field.

169 For each experiment, an instantaneous pulse of 5 to 15 L of 200 $g.L^{-1}$ bromide (in the
170 form of KBr) was injected inside the pollubac at the CW inlet at a flow rate of 4 $L.min^{-1}$ using
171 the pump of an automatic sampler (SD-900 SIGMA) (Table 2).

172 Water was collected at the outlet of both wetlands in two steps: (i) manually sampling
173 approximately every 5 min (from 4 to 9 h, which was chosen according to the nominal HRT,
174 Table 2 and Table A1), and (ii) automatic sampling every 2 h during the subsequent 2 to 5
175 days, until the bromide concentration was believed to be under the limit of quantification
176 (LOQ). These two steps constitute the total sampling period (Table 2). Additionally, spatial
177 water sampling was manually performed by using a telescopic surface water sampler (except
178 for the experiment pond-HF) to determine water pathways (blue numbered circles on Fig. 1),
179 with variable frequencies between 2 min and 30 min (during 4 to 9 h) according to the
180 localization. All samples were collected in a 20 mL clean PE bottle, transported under
181 refrigeration (almost 10°C) to the laboratory and then stored at 4°C prior to analysis.

182 Samples were filtered through a 0.22 µm cellulose acetate filter, and then 1 mL
183 aliquots were transferred to polypropylene vials for analysis with a Dionex ICS-3000 ion
184 chromatographic instrument (Sunnyvale, CA, USA) using Chromeleon® software (version
185 6.80). Concentrations of Br^- were analysed using an AS20 guard column (4 x 50 mm) with a
186 polymeric AS20 analytical column (4 mm x 250 mm). The LOQ was 50 $\mu g.L^{-1}$. Certified
187 standard solutions from Inorganic Ventures (Washington, USA) were used for calibration.
188

189 *2.3. Water transport parameters*
190

To estimate the hydraulic performance of the CWs, water transport parameters were derived from Residence Time Distribution (RTD - corresponding to the bromide restitution curves): the normalized retention time (t_Θ), the effective volume (e_v), the number of cells (N), the hydraulic efficiency (λ), the short-circuiting index (t_{10}/t_n) and the mixing index (t_{90}/t_{10}), were determined. The hydraulic performance is considered good when all of these parameters are optimized, such as when the water is transported from the inlet to outlet circulating in the whole of volume system, which limits the short-circuit.

The normalized hydraulic retention time t_Θ, i.e., the ratio between the mean HRT (t_{mean}) and the nominal HRT (t_n), allows the comparison of RTDs of our 5 tracer experiments. In addition, it corresponds to the effective volume used by water (e_v, characterizing the main channel) (dimensionless) (Fan et al. 2008) allowing to assess the percentage of isolated areas as follows: $(1 - e_v) \times 100$. The nominal HRT (t_n) (h) was calculated as the ratio between the CW volume (m^3) and the flow rate through the CW ($m^3.h^{-1}$); t_{mean}, the mean HRT (h), depicted the average time that the water spent in the system (Eq. (1)):

$$t_{mean} = \frac{\int_0^\infty t\,E(t)\,dt}{\int_0^\infty E(t)dt} \quad (1)$$

where E(t) is the RTD function and is defined by Eq. (2) in the case of pulse injection:

$$E(t) = \frac{C(t)\times Q}{\int C(t)\times Q \times dt} \quad (2)$$

where C(t) is the bromide concentration ($mg.L^{-1}$) at time t, Q is the flow rate ($L.s^{-1}$) at time t and $d_t$is the interval between two consecutive measurements.

The plug flow conditions could be evaluated with the number of cells (N) used in a tank-in-series model (Eq. (3)). Generally, in CWs, the plug flow never occurs, inducing a deviation of the mean HRT (t_{mean}) compared to the nominal HRT (t_n). The higher the N is, the more that the flow is a plug-flow.

$$N = \frac{t_n^2}{\sigma^2} \qquad (3)$$

where σ^2 is a measure of the spread of the RTD and was defined by Eq. (4):

$$\sigma^2 = \frac{\int_0^\infty (t_{mean} - t)^2 E(t) dt}{\int_0^\infty E(t) dt} \qquad (4)$$

The hydraulic efficiency (λ) can be classified as follows: good hydraulic efficiency (λ>0.75), satisfactory hydraulic efficiency (0.5<λ<0.75) and poor hydraulic efficiency (λ<0.5) (Chang et al. 2016).

$$\lambda = t_\theta \left(1 - \frac{1}{N}\right) \qquad (5)$$

Then, short-circuiting and mixing indexes were calculated. Thus, the short-circuiting flow is the situation in which water passes through the CW in less than nominal residence time due to convection process or velocity heterogeneity (Teixeira and Siqueira, 2008). The t_{10}/t_n, defined as the required time to recover 10 % of bromide at the outlet normalized to the nominal HRT t_n,is considered as the value of short-circuit, i.e., the lower the value is, the higher the short-circuit (Guo et al. 2017). The mixing is due to turbulent diffusion and can also be due to recirculation zones and dead zones (Teixeira and Siqueira, 2008). The t_{90}/t_{10} ratio is considered as the value of the mixing index; the larger the value is, the more the mixing flow (Guo et al. 2017), i.e. the t_{90}/t_n was defined as the required time to recover 90 % of bromide at the outlet, normalized to the nominal HRT t_n.

Finally, the Peclet number (Pe) allows distinguishing between the different mixing regimes: convective or dispersive flow; i.e., the lower the Pe value is, the higher the water dispersion (Eq. (6)) (Nameche and Vasel 1998).

$$\mathrm{Pe} = \frac{Q \times L}{W \times Z \times D} \quad (6)$$

where Q is the flow rate ($m^3.h^{-1}$), L is the length of CW (m), W is the width of CW (m), Z is the height of water (m) and D is the dispersion coefficient ($m^2.h^{-1}$) defined by Eq. (7).

$$\mathrm{D} = \alpha \times V_{mean} \quad (7)$$

with α the water dispersivity (m) and V_{mean} ($m.h^{-1}$) the mean water velocity inside the CW (i.e. CW length divided by t_{mean}).

The water dispersivity α was calculated as the mean of two dispersion parameters (dimensionless) which characterized the asymmetrical tracer curve. Those parameters were determined using model.

2.4. TSS measurements and pesticide analysis in water samples

Raw water (water + TSS) was manually sampled during the 2016/2017 hydrological season. For the pond CW, the samples were collected every two weeks from 21/11/16 to 22/05/17 (i.e., 12 samples, 7 under drainage and 5 under no-flow periods). For the ditch CW, samples were collected from 13/02/17 to 13/03/17, due to short drainage season (i.e., 3 samples: 2 under drainage and 1 under a no-flow period).

Water samples were collected at the inlet, at the outlet, in the main channel inside the CW (point MC) and in an isolated area (point IA). Points MC and IA were identified by bromide concentration analysis (MC and IA correspond to points 10 and 9 for the pond CW and 6 and 3 for the ditch CW, respectively) (Fig. 1). Under no-flow, the inlet and outlet sampling was performed in stagnant water close to the inlet and outlet, respectively. All samples were collected in 250 mL PE bottles, which were transported under refrigeration to

the laboratory where they were homogenized and centrifuged at 7000xg and then stored at -20°C until analysis. The electrical conductivity was measured *in situ* for all samples with an electrical probe (HQ40D, HACH-LANGE, France). The analysis of pesticides was performed on an Acquity Ultra-Performance Liquid Chromatography system (UPLC, Waters) interfaced to a triple quadrupole mass spectrometer (Quattro Premier XE, Waters) according to 2 methods: (i) method A was performed to analyse 14 pesticides and 4 metabolites, and (ii) method B was performed to analyse 14 metabolites, as detailed in Table A2. Briefly, for method A, the sample was flushed onto the online SPE cartridge (Oasis HLB 25 µm, 2.1 x 20 mm, Waters) with water (neutral pH). Elution was realized using a gradient of acidified water and acidified acetonitrile (0.05 % formic acid - FA) in the Kinetex 1.7 µm C18 100A (100 x 2.1 mm), Phenomenex. For method B, the sample was flushed onto the online SPE cartouche (Oasis HLB 25 µm, 2.1 x 20 mm, Waters) with acidified water (pH of 3.4). Elution was realized using a gradient of acidified water and acidified acetonitrile (0.007 % FA) in the Kinetex PFP 1.7 µm (100 x 2.1 mm), Phenomenex. The analytical standards were purchased from Cluzeau (Sainte-Foy-La-Grande, France), Restek (Lisses, France), Sigma (Lyon, France), Neochema (Bodenheim, Germany) and Techlab (Metz, France). The limit of quantification ranged from 0.01 to 0.05 $\mu g.L^{-1}$ according to the molecules.

The analyzed pesticides were chosen because of their frequent application in the agricultural plots due to dominant cultures (i.e. winter wheat, rapeseed and maize), and because of their frequent detection in drainage water according to a previous study (Vallée et al. 2015b). Moreover, the diversity of the physico-chemical properties of these molecules (Table A2), allow study the potential contrasted behavior. The metabolites were chosen on the one hand because they are metabolites of widely used pesticides, but rarely studied worldwide; and on the other hand, for their high polarity.

288 To quantify the TSS, 2 L water samples were also manually collected in a 2 L PE
289 bottle. The sampling was performed exclusively at the inlet and outlet due to difficulties in
290 sampling in the MC and IA zones without resuspending the TSS. Then, 250 to 1000 mL of
291 water (depending on particle laden flow) was filtered through 0.7 µm fiber glass filters to
292 separate the largest TSS from the aqueous phase. Before their use, fiber glass filters were
293 cleaned with distilled water, dried at 70°C for 24 h, weighed, and then stored in a glass
294 container. After filtration, filters with the TSS were dried at 70°C for 24 h and then weighed.
295
296 *2.5. Sediment deposition measurement and pesticide concentrations in sediment*
297
298 Sediment deposition was spatially estimated in the pond and ditch CWs (coloured squares on
299 Fig. 1) using PVC cylindrical sediment traps (25 cm high x 5 cm width, H/W ratio of 5) for
300 the 2015/2016 and 2016/2017 hydrological seasons. The sediment traps used in this study
301 allowed for the trapping of the total primary flux of new particles (allochthonously and
302 autochthonously produced) and particles resuspended from the bottom of the wetland, which
303 form the secondary flux (Evans and Håkanson, 1992). Some trap locations were switched
304 from one studied season to another due to the identification of interesting areas based on
305 tracer experiments during the first season (i.e., 2015/2016). Sediment traps were placed in the
306 two CWs before the initiation of drainage in autumn and removed after the drainage season.
307 In the pond CW, sediments were collected during 227 days in 2015/2016 (from 20/11/15 to
308 03/07/2016) and 143 days in 2016/2017 (from 05/11/16 to 27/03/17). In the ditch CW,
309 sediments were collected during 156 days in 2015/2016 (from 04/01/16 to 07/06/16) and 117
310 days in 2016/2017 (from 18/11/16 to 14/03/17).
311 At the laboratory, sediments were recovered from the trap and stored in a pre-weighed
312 250 mL PE bottle. An aliquot of 10 mL was taken after homogenization of the sediment for

313 each sample for particle size estimation. Then, the bottles were stored at -20°C for freeze-
314 drying, and the bottles were weighed. The quantification of sediment in each trap
315 corresponded to the weight difference between the empty and full bottles. The sedimentation
316 rate, i.e., the mass of sediment collected per square centimetre of trap opening per unit of
317 time, was then calculated for each trap (Gardner 1980) for the duration of the drainage season.
318 The particle sizes were measured within 48 h following the sampling using a laser diffraction
319 technique (Helos, Sympatec GmbH), which can measure particle sizes from 0.2 to 90 µm or
320 from 2.4 to 875 µm, according to the chosen lens. In this study, a range from 0.2 to 90 µm
321 was selected due to the fine particle size distribution determined previously. Aliquots of
322 suspended particles of sediment were introduced in the bath-type sonicator integrated with the
323 granulometer and sonicated for 1 min before measurement. Two consecutive measurements of
324 10 seconds, each spaced by 5 seconds, were executed to avoid extreme measurements (i.e.
325 one plant debris measurement was made in the length, biasing the results).

326 Finally, to evaluate the spatial distribution of pesticide concentrations in sediment, a
327 representative sample of each zone (inlet MC, middle MC and outlet MC, and the isolated
328 area) was obtained by mixing four sub-samples. All sub-samples were manually collected in
329 the first upper centimetre of sediment, and in different locations, inside the CW (not in the
330 sediment traps) at the end of each drainage season: in July 2016 for the 2015/2016 season and
331 in April 2017 for the 2016/2017 season. Taking into account the sedimentation rate and its
332 variability, the first centimetre collected can represent one or two years of sedimentation
333 depending on its location in the CW and on the CW. In 2017, a total of four composite
334 samples were collected per CW: 3 samples in the MC zone from inlet to outlet and 1 in the IA
335 zone (point 9 for the pond CW and point 3 for the ditch CW, Fig. 1), whereas only 3 samples
336 in MC were collected in 2016. Indeed, there was no IA zone identified at the beginning of the
337 study in 2016. After sampling, sediments were freeze-dried and then extracted by a modified

QuEChERS (Quick, Easy, Cheap, Effective, Rugged and Safe) method detailed in the SM. Then, they were analysed using one multi-method based on liquid chromatography-electrospray ionization-tandem mass spectrometry (LCeESI-MS/MS) with multiple reaction monitoring described in Vallée et al. (2015). This method allowed the analysis of 67 pesticides and 3 metabolites listed in Table A3.

3. Results and discussion

3.1. Hydrodynamic of the CWs

After the intense sampling time (step 1), the bromide recovery was 77 %, 111 % and 23 % for HF, MF and LF, respectively, in the pond CW and 47 % and 30 % for MF and LF, respectively, in the ditch CW (Table 2). The total sampling period (from 2 to 5 days, step 1 + step 2) allowed a tracer recovery of 104 % for pond-LF and 97 % for ditch-MF. Only 72 % was recovered for the ditch-LF, possibly due to the total sampling period being too short (i.e., bromide was measured up to 0.2 µg/L in the last sample, 5 days after the beginning of the tracer experiment). Finally, the tracer recoveries were always higher than 70 % after the total sampling period (Table 2), so tracer test data can be processed (Lin et al. 2003).

Tracer concentrations as a function of time are shown in Fig. 2, and water transport parameters calculated from RTD data are detailed in Table 3. The nominal HRT (t_n) was longer than the mean HRT (t_m) regardless of the flow rates for the ditch CW and at LF for the pond CW, which suggests short-circuiting for these conditions (Wahl et al. 2010). This is confirmed by the values of short-circuiting (t_{10}/t_n) and mixing indexes (t_{90}/t_{10}) (Table 2). For both CWs, at LF, t_{10}/t_n is lower than at MF and HF, indicating more short-circuiting, and t_{90}/t_{10} is higher than at MF and HF, indicating more water mixing due to higher water

363 dispersion promoted by low flow rates (Guo et al. 2017). Naturally, these results were
364 consistent with the analysis of the number of serial mixing tanks (N), which are lower at LF,
365 indicating that a lower volume of wetland is affected at LF and the hydraulic regime is
366 considered a mixing flow. In addition, the hydraulic efficiency value (λ) was satisfactory at
367 HF and MF in the pond CW (Table 3), whereas it was poor at LF in the pond CW as well as
368 in the ditch CW regardless of the flow rate (Chang et al. 2016). Furthermore, taking all these
369 hydraulic parameters (e_v, N, λ, t_{10}) into account, the hydraulic performance is (i) higher at HF
370 and MF than at LF in the pond CW and (ii) weaker regardless of the flow rate in the ditch
371 CW. Indeed, the flow velocity at the field scale, which is higher for the ditch CW (v_{mean}
372 values from 0.87 to 1.55 m/min) than for the pond CW (v_{mean} values from 0.03 to 0.53
373 m/min), could promote the short-circuiting in the ditch CW, thus decreasing its hydraulic
374 performance. This larger short-circuiting value may be explained by a higher length-to-width
375 ratio for the ditch (80) than for the pond (7), as previously reported by Su et al. (2009). Thus,
376 a linear CW such as our ditch, despite the added enlargement, does not appear to be suitable
377 for retaining water for a long time.

378 Concerning the bromide concentration time series (Fig. 2), for the pond CW, two
379 outlet peaks are identified at LF and MF, indicating two flow paths, while only one peak is
380 visible at HF. This seems to be due to the circulation in pond 3, since only one outlet peak
381 was identified at the outlet of pond 2 (Fig. 3). Indeed, the greater depth of pond 3 (1.2 m
382 compared to 0.5 m in pond 2) could promote deeper water recirculation, inducing two distinct
383 outlet peaks due to a portion of the water being retained and recirculated in this pond. For the
384 ditch CW, only one outlet peak is visible for both flow rates (LF and MF), suggesting that
385 only one major flow path occurred. For both CWs, the outlet peaks appeared slower at LF
386 than at MF or HF (Fig. 2), and this is in agreement with a higher mean HRT at LF (Table 3).
387 In addition, the outlet peaks at LF for the ditch CW and pond CW are wider than those at MF,

suggesting more dispersion here. The presence of isolated areas might contribute to the postponed bromide arrival at the outlet (Fig. 2). The cumulative normalized concentration curves (Fig. 2) provide complementary indications of the water transport processes: the steep slope at the first part of the curve corresponds to convection transport, and the flat part of the curve corresponds to dispersion transport. For the pond CW, the flat part began more rapidly at LF(t_Θ = 0.7) than at HF and MF (t_Θ = 1), indicating more water dispersion at LF, which is in agreement with the t_{90}/t_{10} values (Table 3) and the lower values of the Peclet number (Pe). The lower the Pe value is, the higher the dispersion of water due to low velocity and internal recirculation (Nuel et al. 2017). For the ditch CW, regardless of the flow rate, the flat part begins before t_Θ = 0.5, indicating more dispersion here than in the pond regardless of the flow rate. Moreover, for both CWs, the equilibrium was reached faster at LF than at MF and HF. Thus, for the two CWs, the water transport was dominated by convection at HF and MF and by dispersion at LF (Nuel et al. 2017; Gaullier et al. 2019). Thus, the bromide analysis showed that flow rate influences the water pathways, with a higher proportion of isolated areas at LF (38 % and 89 % for the pond and the ditch, respectively) than at HF or MF (11 % and 68 % for the pond and the ditch, respectively). This corresponds to a volume of isolated areas at LF of 21 m^3 and 20 m^3 for the pond and the ditch, respectively, and at HF or MF of 7-11 m^3 and 26 m^3 for the pond and the ditch, respectively. Thus, the volume of isolated areas inside the ditch CW is quite similar regardless of the flow rate (± 25 %), whereas it is 2 or 3 times higher at LF than at MF/HF in the pond.

3.2. Influence of hydrodynamics on water pathways

To locate the isolated areas, the spatial distribution of the bromide concentration inside both CWs was monitored over time (Fig. 3). To maintain the readability of Fig. 3, only the

413 sampling points in the second pond and the sampling points in the enlargement of the ditch
414 CW were drawn. The supplementary sampling points for the first and the third pond are given
415 in Fig. A1 (Supplementary Material).

416 Focusing on pond 2, at MF, the peak concentration at the outlet (point 12) is lower and
417 more spread out than that at the inlet (point 5), indicating that bromide has circulated from
418 points 5 to 12 by convection and dispersion, corresponding to the main channel. The lower
419 peak concentrations for points 6, 7, 8, 10 and 11 compared to the outlet (point 12) may be
420 explained by a greater transfer of water and tracer by dispersion than by convection from
421 point 5 (Fig. 3). At LF, the concentration peak of bromide was gradually reduced from the
422 inlet (point 5), passing by points 6, 7, 8 and 10, to the outlet (point 12), by convection and
423 dispersion. In addition, all peaks are wider and smaller at LF than at MF, highlighting a
424 greater dispersion due to a water velocity that is ten times slower at LF (Table 3). Point 9 may
425 be considered an isolated area for both flow rates. More precisely, at MF, it was considered a
426 mixing zone due to (i) a more delayed peak time than at the outlet (240 min against 60 min)
427 and (ii) a larger peak than at the outlet, whereas at LF, it was considered a dead zone due to
428 the absence of bromide detection during the tracer experiment. The existence of different
429 hydraulic zones was confirmed by the electrical conductivity distribution measured under
430 seven flow rates inside the pond CW (Fig.4), allowing to generalize the conclusions obtained
431 with the 3 tracer experiments i.e. heterogeneity within the CWs varying according to flow
432 rates. Indeed, regardless of the flow rate, the electrical conductivity measured in the isolated
433 area (point 9, IA zone) is different than that measured in the inlet, main channel (point 10,
434 MC zone) and outlet. Similarly, the electrical conductivity measured in the main channel (MC
435 zone) was almost equal to those measured in the inlet and outlet under drainage. Under the
436 no-flow period, the electrical conductivity measured in the isolated area (point 9, IA zone) is
437 different from that of the main channel (point 10, MC zone) during the first month of no-flow

438 (I, J). Then, beyond this month (K, L), the electrical conductivity becomes similar in the MC
439 and IA zones, which is possibly due to a very slow dispersion during the no-flow period.
440 Concerning the ditch, at MF, peak times of points 2-5-6 and 7 were missed due to the
441 fast flow rate. The main channel path at MF corresponds to the middle of enlargement (points
442 1-5-2-6-7-4). Bromide later reached the border of enlargement (points 8-9-10), and point 3
443 located behind a tuft of *Juncus* (Fig. 3). At LF, the bromide concentration decreased from the
444 inlet to the outlet due to convection and dispersion. The peak times for points 2, 3, 7 and 10
445 are longer than the peak times at the outlet of enlargement (point 4), indicating that these
446 points are clearly affected only by dispersion. Thus, at LF, the main channel was located in
447 the middle of the enlargement and in a part of its left border (5-8-6-9-4). Point 3 could be
448 considered as an isolated area, but not especially a dead zone, as confirmed by the measured
449 electrical conductivity always different at point 3 (corresponding to IA zone, Fig.4) than in
450 the main channel, inlet and outlet (Fig. 4). Finally, points 7 and 10 could be isolated because
451 of their position in the upper corner of the enlargement, as previously suggested by
452 Sabokrouhiyeh et al. (2017). For the pond, all peaks are wider at LF than at MF, highlighting
453 the greater dispersion occurring at LF. The slow water velocity at LF (v_{mean}, Table 3) allowed
454 for the dispersion of water and solutes in the enlargement, increasing the proportion of the
455 isolated area affected by dispersion compared to MF. Otherwise, at MF, the fast water
456 velocity limited the isolated areas (point 3 and the border area, points 8-9-10) affected by
457 dispersion, whereas water was transported by convection in the middle of enlargement.
458 Thus, regardless of the CW, the flow rate influences the water pathways and their
459 geometry. For both CWs, the main channel is globally larger at MF or HF than at LF, and
460 subsequently, the isolated areas are more spread out at LF than at MF or HF.
461
462 *3.3.Influence of hydrodynamics on dissolved pesticide transport*

In the pond CW, among the 32 analysed molecules in the dissolved phase, chlortoluron (CLT), two metabolites of metazachlor (OXA metazachlor, ESA metazachlor) and one metabolite of dimetachlor (CGA 369873) were quantified in the four hydraulic zones (inlet, outlet, MC zone and IA zone) during the 12 sampling campaigns (Table A4, Fig. 5). In the ditch CW, two metabolites of metazachlor (OXA metazachlor, ESA metazachlor) and two metabolites of dimetachlor (OXA dimetachlor, ESA dimetachlor) were quantified in the four hydraulic zones (inlet, outlet, MC zone and IA zone) during the three sampling campaigns (Table A4, Fig. 5).

Under the drainage period, for both CWs, the molecule concentrations are different inside the four zones at a given time, as previously shown with the bromide concentration and electrical conductivity values (Fig.4). No pattern can be highlighted; indeed, pesticide concentrations are sometimes higher in the MC zone and sometimes higher in the IA zone, except for cases G and H in the pond CW. For these two cases, where LF is preceded by MF, the molecule concentrations measured in the IA zone (point 9) are always lower than those in the MC zone (point 10). These results may be explained by a higher mitigation in IA (adsorption in sediments and degradation) and/or a limited water dispersion inside IA. It should also be kept in mind that water entering the CW has a time-dependent composition. In contrast, the concentrations for all MC points (MC + inlet + outlet) are always quite similar for a given sampling campaign, indicating limited pesticide removal from the inlet to outlet. The few data collected in the ditch (3 samples) limit the ability to draw conclusions for this CW. In conclusion, pesticide concentrations are heterogeneous in the CW during drainage, regardless of whether there are high or low flow rates.

Under the no-flow period, the concentrations of pesticides in the pond (cases I to L), measured in the MC and IA zones, are close, especially after one month of no-flow (Fig. 5).

488 This observation is consistent with the electrical conductivity values previously described as
489 homogeneous during this no-flow period (Fig. 4). Dispersion is the dominant transport under
490 the no-flow period and slowly leads to a uniform contaminant distribution inside the CW. The
491 distance travelled by diffusion is only approximately 1 cm per day for a molecule (Gaullier et
492 al. 2018). Thus, considering a distance of 2 m from MC to IA, more than 200 days would be
493 necessary for a whole homogenization of the water volume by diffusion. Nevertheless, the
494 homogenization took place in less than one month, which suggests that other processes than
495 diffusion take place, such as wind mixing, vegetation patterns, and bioturbation, as previously
496 observed by Werner and Kadlec (2000) and Zounemat-Kermani et al. (2015).
497 In conclusion, the dissolved pesticide concentrations show spatial heterogeneity during the
498 drainage phases (LF or MF) (in agreement with the bromide monitoring and conductivity) and
499 during homogenization of the concentrations in the constructed wetland after one month of no
500 flow. On the other hand, no link could be highlighted between the pesticide concentrations
501 and the flow rate or the water pathways.
502
503 3.4. *Influence of hydrodynamics on the sedimentation rate*
504
505 In addition to being transported by the dissolved phase, pesticides can be transported by the
506 particulate phase via the suspended solids entering the CW via tile drains. The TSS
507 transported by drainage entering the pond CW was 1500 kg in 2016 (75 $kg.ha^{-1}.y^{-1}$ or 7.8
508 $kg.day^{-1}$) and 400 kg in 2017 (20 $kg.ha^{-1}.y^{-1}$ or 4.8 $kg.day^{-1}$). In the ditch CW, the TSS
509 entering was 780 kg in 2016 (78 $kg.ha^{-1}.y^{-1}$ or 8.3 $kg.day^{-1}$) and 300 kg in 2017 (30 $kg.ha^{-1}.y^{-1}$
510 or 8.8 $kg.day^{-1}$) (Fig. A2). The lower exportation in 2017 than in 2016 may be due in part to a
511 smaller total drained volume in 2017 (23920 m^3 and 2960 m^3 in the pond and the ditch,
512 respectively) than in 2016 (83530 m^3 and 10475 m^3 in the pond and the ditch, respectively).

513 To understand the transport and fate of solid-bound pesticides inside the CW, we focused on
514 the spatial repartition of pesticide concentrations in sediments, whereas sedimentation is the
515 main process of mitigation for solid-bound pesticides inside the CW, as previously shown by
516 Koskiaho (2003).

517 The spatial distribution of the sedimentation rate is shown in Fig. 6. The annual
518 sediment accumulation in the pond varied from 1.4 to 8 $kg.m^{-2}.y^{-1}$ (0.2 to 1 $cm.yr^{-1}$) in the
519 main channel (T1 to T4), varied from 0.47 to 2.9 $kg.m^{-2}.y^{-1}$ (0.1 to 0.4 $cm.yr^{-1}$) in the border
520 area (T5 to T8), and was 4.2 $kg.m^{-2}.y^{-1}$ (0.5 $cm.yr^{-1}$) in the isolated area (T9). For the ditch, the
521 sediment accumulation varied from 2 to 12.7 $kg.m^{-2}.y^{-1}$ (0.5 to 1.6 $cm.yr^{-1}$) in the main
522 channel (T1 to T3), from 1 to 2.5 $kg.m^{-2}.y^{-1}$ (0.1 to 0.3 $cm.yr^{-1}$) in the border area (T4 to T6),
523 and between 4.6 and 5.4 $kg.m^{-2}.y^{-1}$ (0.6 and 0.7 $cm.yr^{-1}$) in the two isolated areas (T7 and T8,
524 respectively) (Fig. 6). These sedimentation rates are in accordance with those of Fennessy et
525 al. (1994) who reported rates from 5.9 to 12.8 $kg.m^{-2}.y^{-1}$. For both CWs, the lower
526 sedimentation rates in the border areas than in the MC may be due to an emergence of border
527 traps during low flow rates (T5 to T8 in the pond CW and T4 to T6 in the ditch CW). In
528 addition, the sedimentation rate in MC and IA is almost equal despite a possible greater water
529 volume passing through the MC than through the IA. This result may be explained by a higher
530 resuspension of sediment in the MC than in the IA due to a faster water velocity. This process
531 of resuspension was highlighted (i) by a relatively uniform spatial distribution of sediment
532 particle size inside the CW (Fig. A3) and (ii) by the greater amount of particles settled in both
533 CW traps than the amount of particles reaching the inlet (Fig. A2).

534 Dimetachlor (DMT) was the single quantified pesticide reaching the CWs by
535 particulate phase only (data not shown) and was also quantified in sediments (Fig. 7). For
536 both CWs, the DMT concentrations in sediment were similar regardless of the sampling zone
537 (Fig. 7), which corroborates the uniform sedimentation inside the CW and even in the isolated

538 area. Thus, the isolated areas can also mitigate solid-bound pesticides by sedimentation.
539 Otherwise, the resuspension of sediments from the main channel could induce a release of
540 solid-bound pesticides towards the CW outlet, which could lead to a negative mitigation rate
541 of solid-bound pesticides.
542
543 *3.5. Influence of hydrodynamics on the spatial distribution of the pesticide levels in*
544 *sediments*
545 Concerning the pesticides reaching the CW by dissolved phase only (data not shown),
546 their quantification onto the sediments indicated their adsorption from the dissolved phase,
547 which is the case for epoxyconazole (EPX) in the pond and cyproconazole (CYP) and
548 metconazole (MCZ) in the ditch (Fig. 7). No metabolites were quantified in the sediments,
549 possibly due to their high polarity properties.
550 For the pond sediment, the EPX concentration is higher in the IA (point 9) than in the
551 MC (ponds 1, 2 and 3). This higher pesticides storage in sediments in IA than MC could be
552 due to: (i) adsorption process of EPX favoured by the dispersion transport in IA, (ii) or/and
553 due to desorption process which could be favoured in MC due to convection transport as
554 previously shown in Gaullier et al. (2018); (iii) or/and due to degradation process, favoured in
555 MC. In the same manner, Schuetz et al. (2012) also showed that adsorption was higher in IA
556 (dead zones in their study) compared to zones where convection was dominant, such as the
557 MC in our study.
558 In the ditch sediment, the CYP and MCZ concentrations were lower in the IA (point 3)
559 than in the MC (inlet, outlet and enlargement) (Fig. 7). This contradictory observation when
560 compared with the pond could be due to the location of the IA. Indeed, the IA was located in
561 the border area of the ditch and sometimes emerged during low flow rates, whereas in the
562 pond, the IA never emerged.

563 Finally, favourable hydraulic conditions, as shown in isolated areas (slow water
564 velocity, long HRT), could increase the mitigation of dissolved pesticides inside the CW by
565 adsorption on sediment, as demonstrated in the results.
566
567 **Conclusion**
568 Bromide tracing and electrical conductivity monitoring allowed us to identify and delineate
569 two water pathways (or hydraulic zones) inside the CWs: the main channel with water
570 transported mainly by convection and the isolated areas with water transported by dispersion.
571 The area and the location of these hydraulic zones fluctuate according to the flow rate. For the
572 ditch and pond, the proportion of isolated areas is greater at low flow rates (0.5 L/s,
573 representing 50 % of annual flow rates) than at medium or high flow rates (4-7 L/s,
574 representing 10 % of annual flow rates). During drainage, these different water pathways led
575 to a heterogeneous distribution of dissolved pesticide concentrations inside the CW, as
576 illustrated for the aqueous phase and the adsorbed pesticide concentrations on sediment. This
577 heterogeneity between the main channel and the isolated areas is more notable at low flow
578 than at high flow in the short term, since isolated areas are affected later by dispersion at LF
579 than at HF. In the long term, this heterogeneity disappears during the no-flow phase due to the
580 dispersion of pesticides and metabolites inside the CWs. Pesticides entering the CW that are
581 adsorbed on TSS are mitigated by sedimentation. The sedimentation rates are quite similar
582 between the main channel and the isolated areas, whereas the isolated areas are (i) less
583 affected by water than the main channel, (ii) less impacted by resuspension of sediments than
584 the main channel and (iii) sometimes emerged (for the ditch). In addition, analyses of
585 pesticides reaching the CW inlet in the dissolved phase only showed that storage in the
586 sediments seems favoured in the isolated areas compared to the main channel. These isolated
587 areas appear effective for dissolved and particulate pesticide mitigation, especially

588 considering a complete drainage season. Finally, fine-time field monitoring is needed to
589 determine the pesticide mitigation effectiveness of CWs at different temporal scales.
590
591
592 **Acknowledgements**
593
594 This research received financial support from the Rhin Meuse Water Agency contract
595 n°14A54005, BRGM (French Geological Survey), the University of Lorraine, the FEDER-
596 FSE Lorraine and Massif des Vosges (Fonds Européens de DEveloppement Regional – Fond
597 Social Européen) and the Moselle Basin LTSER. The authors thank J-S. PY (LHN, Nancy)
598 and E. Coisy (BRGM, Orléans) for their helpful laboratory assistance, the farmers and R.
599 Cherrier and F.X. Schott (Chambre Régionale d'Agriculture du Grand Est) for field access.
600 The authors also thank C. Gauthier and V. Dutreuil for drone shooting and D. Billet, A. de
601 Junet, S. Nachin, L. Staedelin, R. Gley and M. Dincher for their helpful sampling work during
602 the tracer tests experiments, and A. Recouvreur and G. Pecheux for their work on
603 the CW topography measurement.

References

Alvord, H., Kadlec, R., 1996. Atrazine fate and transport in the Des Plaines Wetlands. Ecol. Model. 90, 97–107.

Chang, T-J., Chang, Y-S., Lee, W-T., Shih, S-S., 2016. Flow uniformity and hydraulic efficiency improvement of deep-water constructed wetlands. Ecol. Eng. 92, 28–36.

Elsaesser, D., Blankenberg, A-G.B., Geist, A., Mæhlum, T., Schulz, R., 2011. Assessing the influence of vegetation on reduction of pesticide concentration in experimental surface flow constructed wetlands: Application of the toxic units approach. Ecol. Eng. 37, 955-962.

Elsayed, O.F., Maillard, E., Vuilleumier, S., Imfeld, G., 2014. Bacterial communities in batch and continuous-flow wetlands treating the herbicide S-metolachlor. Sci. Total Environ. 499, 327-335.

Evans, R.D., Håkanson, L., 1992. Measurement and prediction of sedimentation in small Swedish lakes. Hydrobiologia 235-236, 143–152.

Fan, L., Reti, H., Wang, W., Lu, Z., Yang, Z., 2008. Application of computational fluid dynamic to model the hydraulic performance of subsurface flow wetlands. J. Environ. Sci. 20, 1415-1422.

Fennessy, M., Brueske, C.C., Mitsch, W.J., 1994. Sediment deposition patterns in restored freshwater wetlands using sediment traps. Ecol. Eng. 3, 409-428.

Gardner, W., 1980. Sediment trap dynamics and calibration: a laboratory evaluation. J. Mar. Res. 38, 17-39

627 Gaullier, C., Dousset, S., Billet, D., Baran, N., 2018. Is pesticide sorption by constructed
628 wetland sediments governed by water level and water dynamics? Environ. Sci. Pollut.
629 Res. 25, 14324-14335.
630 Gaullier, C., Baran, N., Dousset, S., Devau, N., Billet, D., Kitzinger, G., Coisy, E., 2019.
631 Wetland hydrodynamics and mitigation of pesticides and their metabolites at pilot-
632 scale. Ecol. Eng. 136, 185-192.
633 Gregoire, C., Elsaesser, D., Huguenot, D., Lange, J., Lebeau, T., Merli, A., Mose, R.,
634 Passeport, E., Payraudeau, S., Schütz, T., Schulz, R., Tapia-Padilla, G., Tournebize, J.,
635 Trevisan, M., Wanko, A., 2009. Mitigation of agricultural nonpoint-source pesticide
636 pollution in artificial wetland ecosystems. Environ. Chem. Lett. 7, 205-231.
637 Guo, C., Cui Y., Dong B., Luo, Y., Liu, F., Zhao, S., Wu, H., 2017. Test study of the optimal
638 design for hydraulic performance and treatment performance of free water surface
639 flow constructed wetland. Bioresource Technol. 238, 461-471.
640 Jenkins, G.A., Greenway, M., 2005. The hydraulic efficiency of fringing versus banded
641 vegetation in constructed wetlands. Ecol. Eng. 25, 61-72.
642 JOCE, 2000. Directive 2000/60/EC of the European Parliament and of the Council of 23
643 October 2000 Establishing a Framework for Community Action in the field of Water
644 Policy, L337.
645 JOCE, 2006. Directive 2006/118/EC of the European Parliament and the Council of 12
646 December 2006 on the Protection of Groundwater against Pollution and Deterioration,
647 L372.
648 Kadlec, R.H., 1994. Detention and mixing in free water wetlands. Ecol. Eng. 3, 345-380.
649 Koskiaho, J., 2003. Flow velocity retardation and sediment retention in two constructed
650 wetland–ponds. Ecol. Eng. 19, 325–337.

651 Lewis, K.A., Tzilivakis, J., Warner, D., Green, A.,2016. An international database for
652 pesticide risk assessments and management. Human and Ecological Risk Assessment:
653 Internat. J. 22, 1050-1064.
654 Lin, A.Y-C., Debroux, J-F., Cunningham, J.A., Reinhard, M., 2003. Comparison of
655 rhodamine WT and bromide in the determination of hydraulic characteristics of
656 constructed wetlands. Ecol. Eng. 20, 75-88.
657 Liu, J.J., Dong, B., Guo, C.Q., Liu, F.P., Brown, L., Li, Q., 2016. Variations of effective
658 volume and removal rate under different water levels of constructed wetland. Ecol.
659 Eng. 95, 652-664.
660 Liu T, Xu S, Lu S, Qin P, Bi B, Ding H, Liu Y, Guo X, Liu X. 2019. A review on removal of
661 organophosphorus pesticides in constructed wetland: Performance, mechanism and
662 influencing factors.Sci. Total Environ. 651, 2247-2268.
663 Maillard, E., Payraudeau, S., Ortiz, F., Imfeld, G., 2011. Removal of dissolved pesticide
664 mixtures by a stormwater wetland receiving runoff from a vineyard catchment: An
665 inter-annual comparison.Int. J. Environ. An. Chem. 92, 1-16.
666 Maillard E, Imfeld G (2014) Pesticide Mass Budget in a Stormwater Wetland. Environmental
667 Science & Technology 48:8603–8611.
668 Martinez, C.J., Wise, W.R., 2003. Hydraulic analysis of Orlando easterly wetland. J. Environ.
669 Eng. 129, 553-560.
670 Matamoros, V., García, J., Bayona, J.M., 2008. Organic micropollutant removal in a full-scale
671 surface flow constructed wetland fed with secondary effluent. Water Res. 42, 653-660.
672 Moore, M.T., Bennett, E.R., Cooper, C.M., Smith, S., Shields, F.D., Milam, C.D., Farris, J.L.,
673 2001. Transport and fate of atrazine and lambda-cyhalothrin in an agricultural
674 drainage ditch in the Mississippi Delta, USA. Agric. Ecosyst. Environ. 87, 309-314.

675 Moore, M.T., Tyler, H.L., Locke, M.A., 2013. Aqueous pesticide mitigation efficiency of
676 *Typha latifolia (L.), Leersia oryzoides (L.) Sw., and Sparganium americanum Nutt.*
677 Chemosphere 92, 1307-1313.
678 Nameche, T.H, Vasel, J.L., 1998. Hydrodynamic studies and modelization for aerated lagoons
679 and waste stabilization ponds. Water res. 32, 3039-3045.
680 Nuel, M., Laurent, J., Bois, P., Heintz, D., Mosé, R., Wanko, A., 2017. Seasonal and ageing
681 effects on SFTW hydrodynamics study by full-scale tracer experiments and dynamic
682 time warping algorithms. Chem. Eng. J. 321, 86-96.
683 Sabokrouhiyeh, N., Bottacin-Busolin, A., Savickis, J., Nepf, H., Marion, A., 2017. A
684 numerical study of the effect of wetland shape and inlet-outlet configuration on
685 wetland performance. Ecol. Eng. 105, 170-179.
686 Schuetz, T., Weiler, M., Lange, J., 2012., Multitracer assessment of wetland succession:
687 Effects on conservative and non-conservative transport processes. Water Resour. Res.
688 48, 1-15.
689 Schultz, R.C., Collettil, J.P., Isenhart, T.M., Simpkins, W.W., Mize, C.W., Thompson, M.L.,
690 1995. Design and placement of a multi-species riparian buffer strip system.
691 Agroforest. Syst. 29, 201-226.
692 Shih, S., Zeng, Y., Lee, H., Otte, M., Fang, W., 2017. Tracer Experiments and Hydraulic
693 Performance Improvements in a Treatment Pond. Water 9, 137.
694 Stehle, S., Elsaesser, D., Gregoire, C., Imfeld, G., Niehaus, E., Passeport, E., Payraudeau, S.,
695 Schäfer, R.B., Tournebize, J., Schulz, R., 2011. Pesticide Risk Mitigation by
696 Vegetated Treatment Systems: A Meta-Analysis. J. Environ. Qual. 40, 1068-1080.
697 Su, T-M., Yang, S-C., Shih, S-S., Lee, H-Y., 2009. Optimal design for hydraulic efficiency
698 performance of free-water-surface constructed wetlands. Ecol. Eng. 35, 1200-1207.

699 Thackston, E.L., Shields, D. Jr., Schroeder P.R., 1987. Residence time distributions of
700 shallow basins. J. Environ. Eng. 113, 1319-1332.
701 Teixeira, E.C., Siqueira, R.D.N., 2008. Performance assessment of hydraulic efficiency
702 indexes. J. Environ. Eng. 134, 851–859
703 Tournebize, J., Gramaglia, C., Birmant, F., Bouarfa, S., Chaumont, C., Vincent, B., 2012. Co-
704 design of constructed wetlands to mitigate pesticide pollution in a drained catch-basin:
705 a solution to improve groundwater quality. Irrig. Drain. 61, 75-86.
706 Vallée R, Dousset S, Billet D (2015a). Water residence time and pesticide removal in pilot-
707 scale wetlands. Ecological Engineering 85:76–84.
708 Vallée, R., Dousset, S., Schott, F.-X., Pallez, C., Ortar, A., Cherrier, R., Munoz, J.-F., Benoît,
709 M., 2015b. Do constructed wetlands in grass strips reduce water contamination from
710 drained fields? Environ. Pollut. 207, 365-373.
711 Vymazal, J., Březinová, T., 2015. The use of constructed wetlands for removal of pesticides
712 from agricultural runoff and drainage: A review. Environ. Int. 75, 11-20.
713 Wahl, M.D., Brown, L.C., Soboyejo, A.O., Martin, J., Dong, B., 2010. Quantifying the
714 hydraulic performance of treatment wetlands using the moment index. Ecol. Eng. 36,
715 1691-1699.
716 Werner, T.M., Kadlec, R.H., 2000. Wetland residence time distribution modeling. Ecol. Eng.
717 15, 77-90.
718 Zounemat-Kermani, M., Scholz, M., Tondar, M-M., 2015. Hydrodynamic modelling of free
719 water-surface constructed storm water wetlands using a finite volume technique.
720 Environ. Technol. 36, 2532-2547.
721
722

Figure captions

Figure 1. Location of the sampling points in photographs taken by a drone (5 November 2018) of the two-constructed wetlands: a succession of three ponds (A) and a ditch (B)

Figure 2. Tracer breakthrough curves and cumulative normalized tracer concentrations ($F(t) = \sum E(t) \times dt$) under various flow rates (HF: high flow, MF: mean flow, LF : low flow) for both wetlands (pond and ditch)

Figure 3. Spatial distribution of bromide concentration versus time under various flow rates (LF: low flow, MF: mean flow) in the second pond and ditch

Figure 4. Electrical conductivity (µS/cm) in the inlet, outlet, main channel (MC) and isolated area (IA) zones under distinct flow rates (HF: high flow, LF: low flow, MF: mean flow and no flow) for the pond and ditch

Figure 5. Pesticide concentrations (µg/L) in the inlet, outlet, main channel (MC) and isolated area (IA) zones under distinct flow rates (HF: high flow, LF: low flow, MF: mean flow and no flow) for the pond and ditch

Figure 6. Spatial distribution of sedimentation rate within the pond and the ditch (MC: main channel, border, IA: isolated area) for the different sediment traps (numbered T1 to T9)

747 **Figure 7.** Pesticide concentrations (µg/kg) in sediments collected at the end of the 2016/2017
748 drainage season for pesticide entering CW by dissolved phase (EPX: epoxyconazole, CYP:
749 cyproconazole, MCZ: metconazole) and by particulate phase (DMT: dimetachlor)

Table captions

Table 1. Meteorological, hydrological and agricultural datas characterizing the two studied constructed wetlands

Table 2. Tracer experiment parameters and hydraulic characteristics of the pond and the ditch under various flow rates for the pond and ditch

Table 3. Transport parameters derived from the Residence Time Distribution analysis for the pond and ditch under distinct flow rates

Figure captions

Figure 1. Location of the sampling points in photographs taken by a drone (5 November 2018) of the two-constructed wetlands: a succession of three ponds (A) and a ditch (B)

Figure 2. Tracer breakthrough curves and cumulative normalized tracer concentrations ($F(t) = \sum E(t) \times dt$) under various flow rates (HF: high flow, MF: mean flow, LF : low flow) for both wetlands (pond and ditch)

Figure 3. Spatial distribution of bromide concentration versus time under various flow rates (LF: low flow, MF: mean flow) in the second pond and ditch

Figure 4. Electrical conductivity (µS/cm) in the inlet, outlet, main channel (MC) and isolated area (IA) zones under distinct flow rates (HF: high flow, LF: low flow, MF: mean flow and no flow) for the pond and ditch

Figure 5. Pesticide concentrations (µg/L) in the inlet, outlet, main channel (MC) and isolated area (IA) zones under distinct flow rates (HF: high flow, LF: low flow, MF: mean flow and no flow) for the pond and ditch

Figure 6. Spatial distribution of sedimentation rate within the pond and the ditch (MC: main channel, border, IA: isolated area) for the different sediment traps (numbered T1 to T9)

Figure 7. Pesticide concentrations (µg/kg) in sediments collected at the end of the 2016/2017 drainage season for pesticide entering CW by dissolved phase (EPX: epoxyconazole, CYP: cyproconazole, MCZ: metconazole) and by particulate phase (DMT: dimetachlor)

Table captions

Table 1. Meteorological, hydrological and agricultural datas characterizing the two studied constructed wetlands.

Table 2. Tracer experiment parameters and hydraulic characteristics of the pond and ditch under various flow rates for the pond and ditch

Table 3. Transport parameters derived from the Residence Time Distribution analysis for the pond and ditch under distinct flow rates

Figure 1. Location of the sampling points in photographs taken by a drone (5 November 2018) of the two-constructed wetlands: a succession of three ponds (A) and a ditch (B)

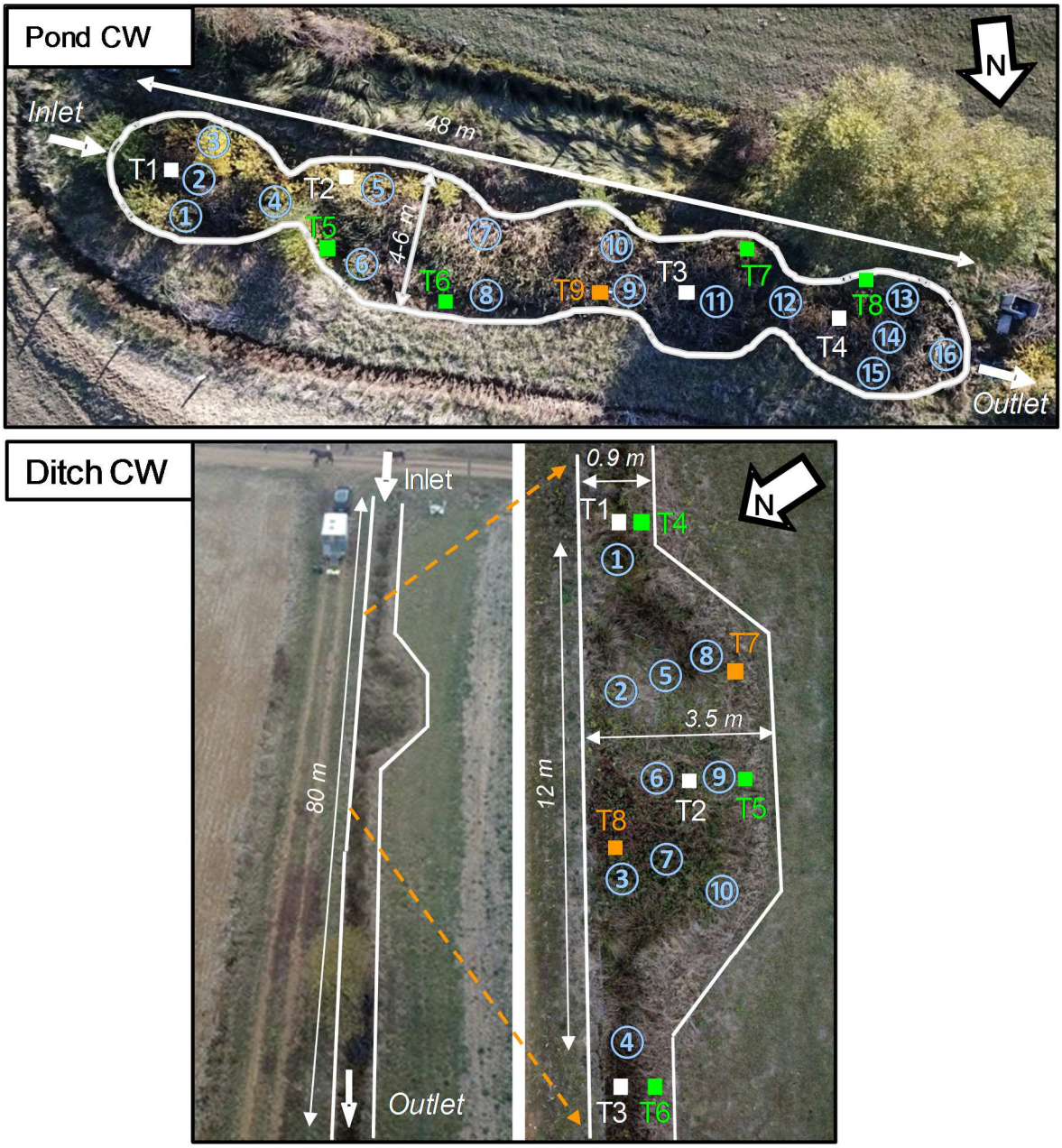

Blue numbered circles correspond to the manual water sampling during the bromide tracing.

Coloured squares correspond to the location of sediment traps: white for the main channel, green for the borders and orange for isolated areas.

Figure 2. Tracer breakthrough curves and cumulative normalized tracer concentrations ($F(t) = \sum E(t) \times dt$) under various flow rates (HF: high flow, MF: mean flow, LF : low flow) for both wetlands (pond and ditch)

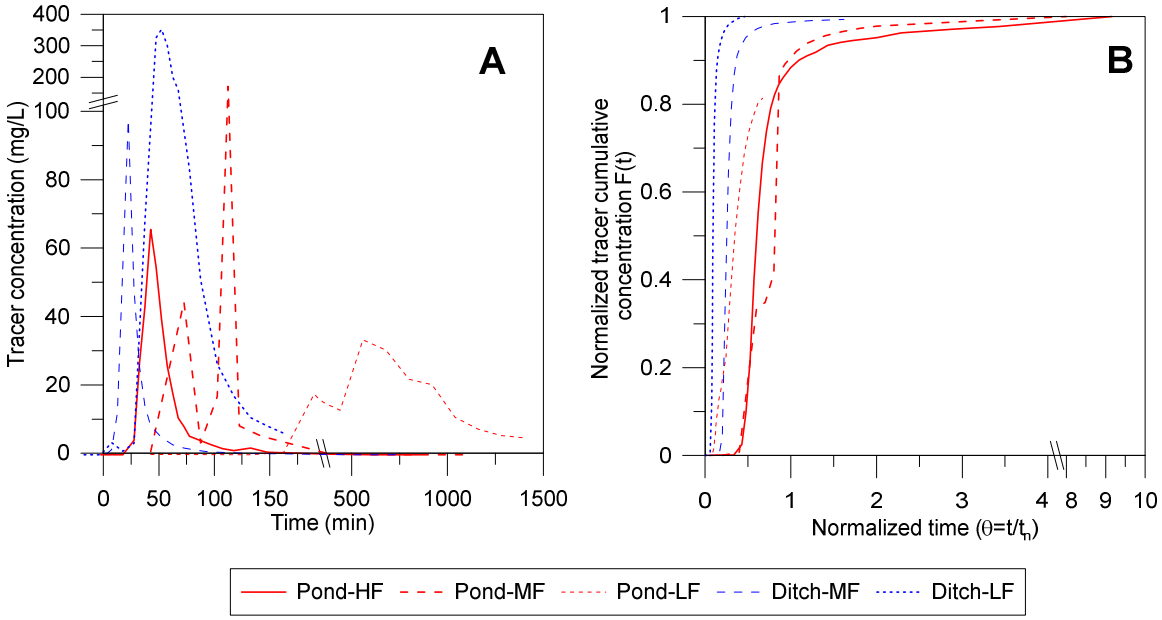

Figure 3. Spatial distribution of bromide concentration versus time under various flow rates (LF: low flow, MF: mean flow) in the second pond and ditch

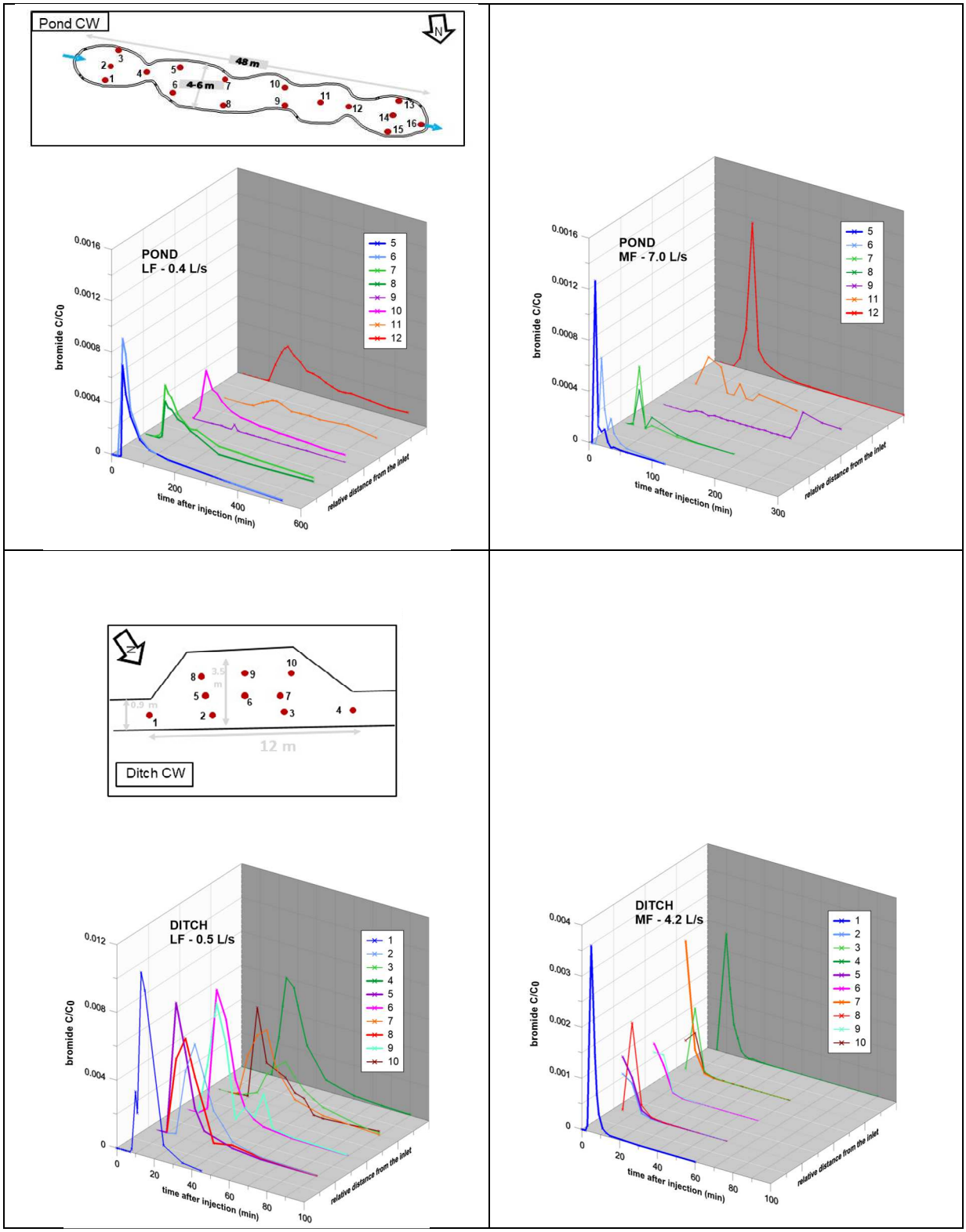

In the pond, point 10 was not sampled at MF (7 L/s), and there is no associated curve on the graph.

Figure 4. Electrical conductivity (µS/cm) in the inlet, outlet, main channel (MC) and isolated area (IA) zones under distinct flow rates (HF: high flow, LF: low flow, MF: mean flow and no flow) for the pond and ditch

Each letter (from A to L) corresponds to one sampling date.

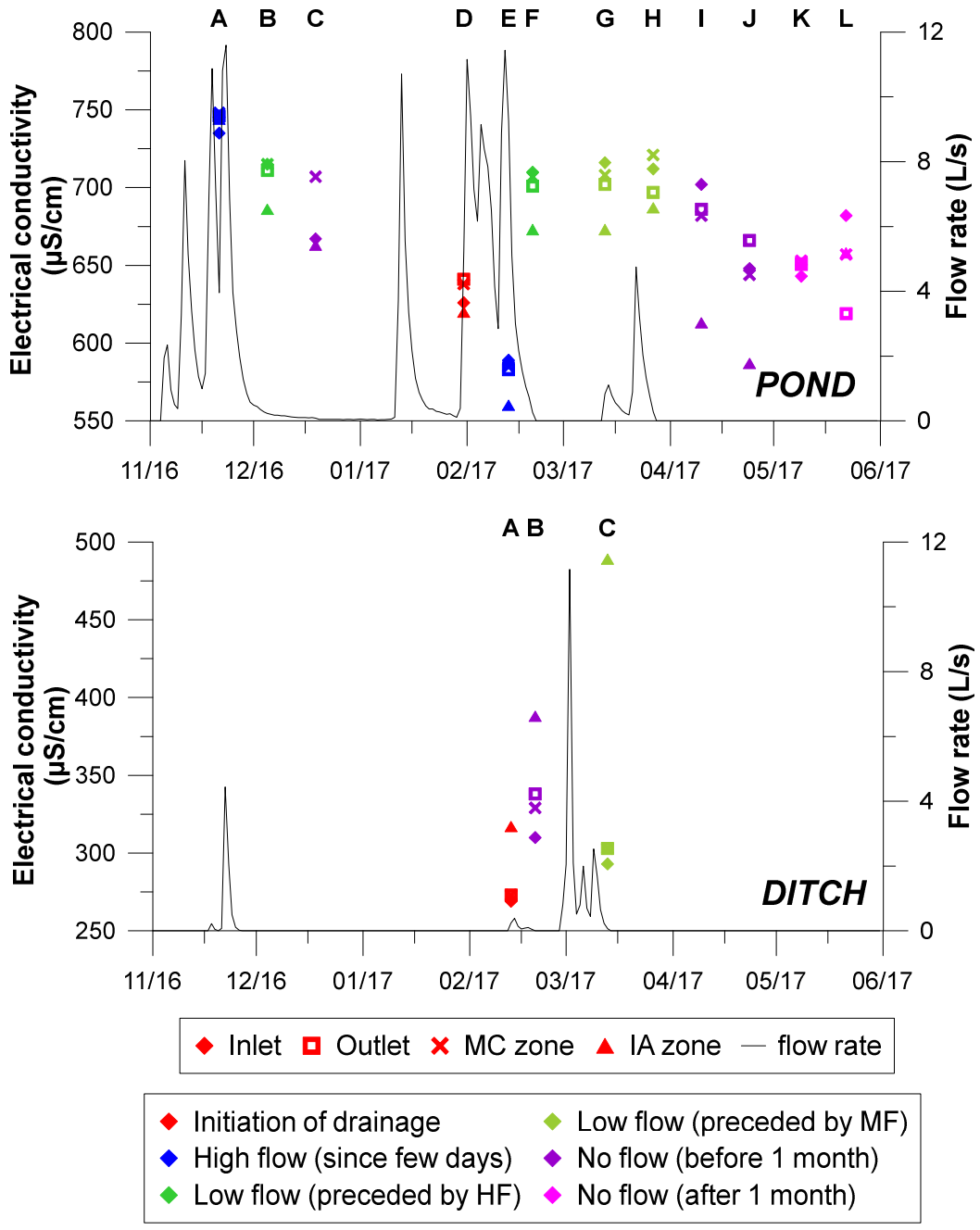

For the pond, the MC zone was collected in point 10, and the IA zone was collected in point 9. For the ditch, the MC zone was collected in point 6, and the IA zone was collected in point 3 (Figure 3).

Figure 5. Pesticide concentrations (µg/L) in the inlet, outlet, main channel (MC) and isolated area (IA) zones under distinct flow rates (HF: high flow, LF: low flow, MF: mean flow and no flow) for the pond and ditch

Each letter (from A to L) corresponds to one sampling date.

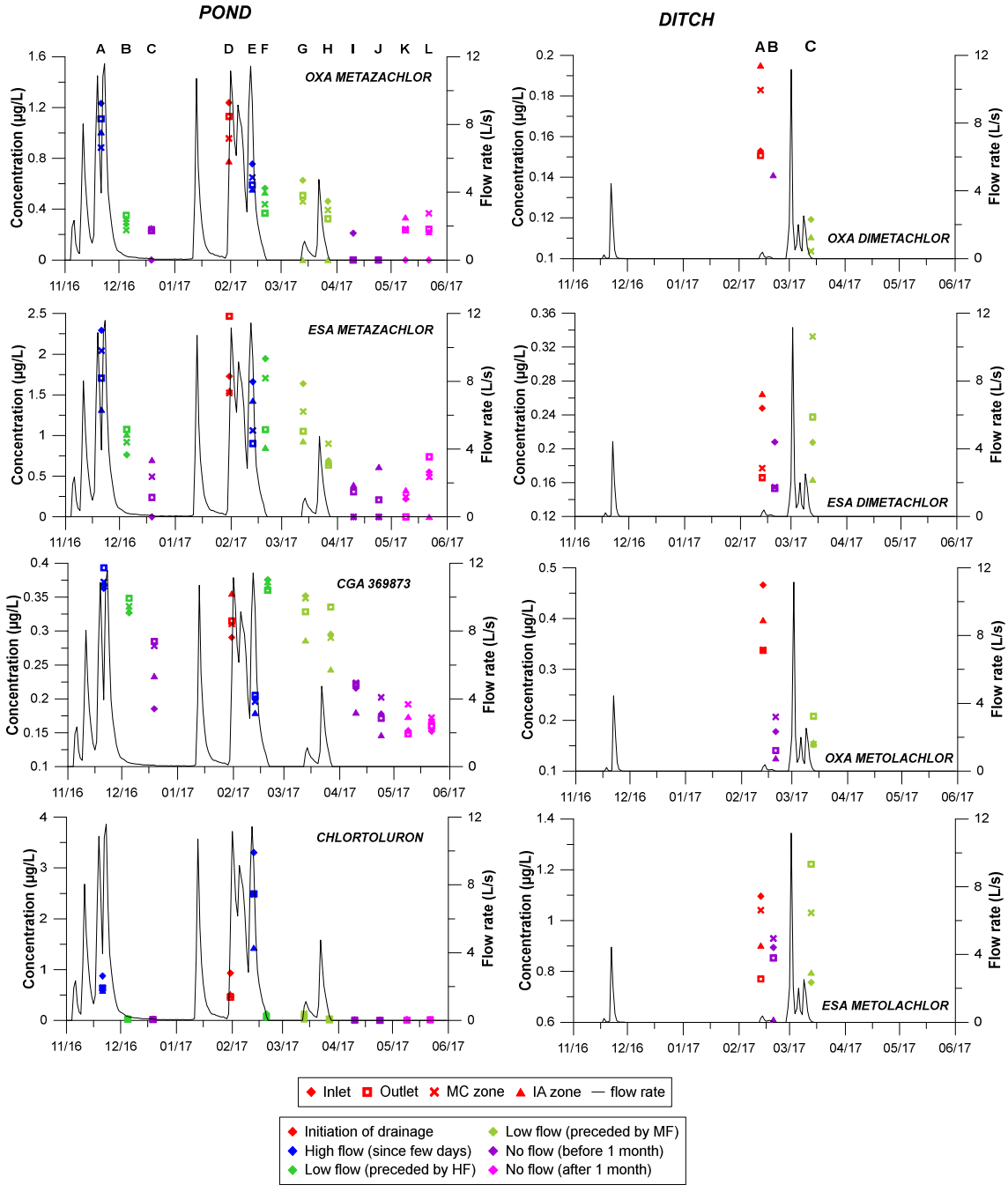

For the pond, the MC zone was collected in point 10, and the IA zone was collected in point 9. For the ditch, the MC zone was collected in point 6 and the IA zone was collected in point 3 (Figure 3).

Figure 6. Spatial distribution of sedimentation rate within the pond and the ditch (MC: main channel, border, IA: isolated area) for the different sediment traps (numbered T1 to T9)

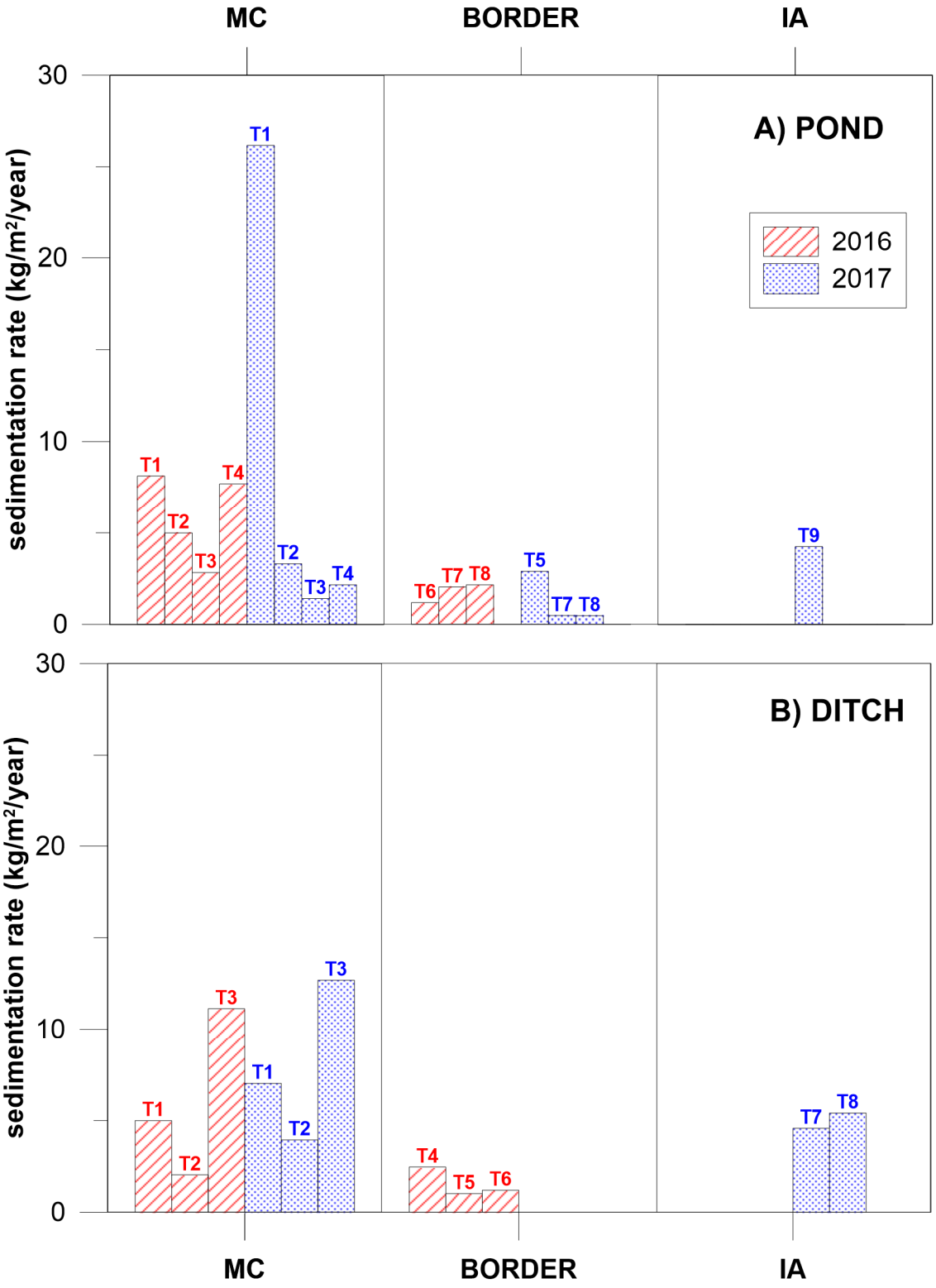

Figure 7. Pesticide concentrations (µg/kg) in sediments collected at the end of the 2016/2017 drainage season for pesticide entering CW by dissolved phase (EPX: epoxyconazole, CYP: cyproconazole, MCZ: metconazole) and by particulate phase (DMT: dimetachlor)

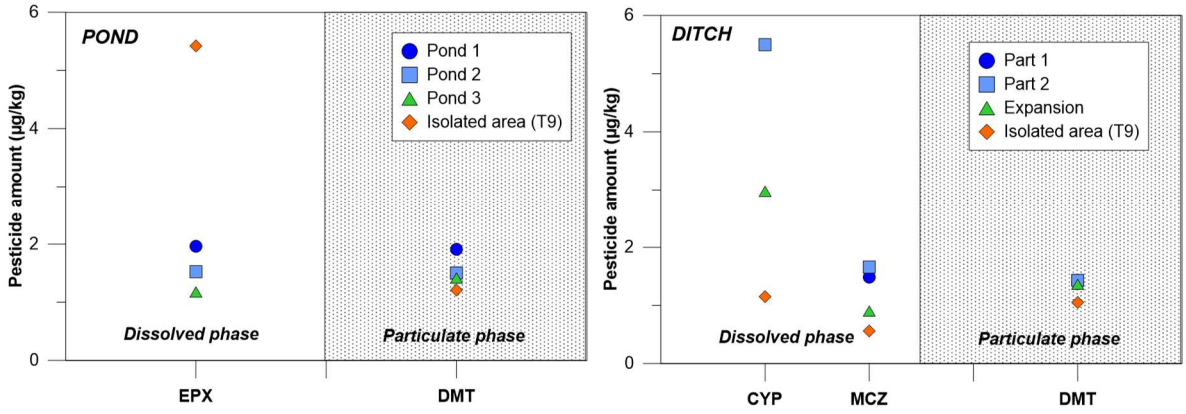

Table 1. Meteorological, hydrological and agricultural data characterizing the two studied constructed wetlands.

Crop rotation	Rainfall* (mm/d)	30-yr average rainfall* (mm/d)	Inlet volume* (mm/d)	Flow rate variation* (L/s)	Flow distribution	HRT* (h)	Drainage period* (d)	Dry period* (d)
				POND				
barley/rape/ winter wheat	1.9 - 3.2	2.7	2 - 4.5**	0.2 - 21.5	<2 L/s : 50% 2-7 L/s : 25% >7 L/s : 25%	1 - 40	7 - 43	2 - 37
				DITCH				
rape/winter wheat/maize/ winter wheat	1.9 - 3.5	2.3	0.3 - 0.7	0.01 - 11	<0.2 L/s : 50% 0.2-1 L/s : 25% 1-4 L/s : 21% >4 L/s : 4%	1 - 181	4 - 54	2 - 75

* From the beginning (November) to the end of drainage (March-April) during 3 drainage seasons (2014-2017).

**The drained volume higher than total rainfall might be due to runoff from an adjacent plot.

Table 2. Tracer experiment parameters and hydraulic characteristics of the pond and ditch under various flow rates for the pond and ditch

Tracer test name*	Pond-HF	Pond-MF	Pond-LF	Ditch-MF	Ditch-LF
Injection date	15/02/2016	13/06/2016	15/03/2017	01/04/2016	08/03/2017
Injected volume (L)	15	10	10	5	5
Sampling time** (step 1) (h)	7	5	9	4	6
Total sampling period*** (step 1 + step 2) (h)	48	48	96	48	120
Restitution after sampling time (%)	77	111	23	47	30
Restitution after total sampling period (%)	77	111	104	97	72
Mean flow rate (L/s)	13.0 ± 0.4	8.0 ± 0.3	0.6 ± 0.2	4.0 ± 0.9	0.34 ± 0.02
Water depth (m)****	0.18/0.34/0.48	0.08/0.25/0.35	0.05/0.20/0.31	0.15/0.10/0.35	0.10/0.05/0.21
Volume of wetland (m^3)	83	63	55	38	23
Water temperature (°C)	8	12	9	8	6
Electrical conductivity (µS/cm)	530	625	700	210	295
pH(µS/cm)	6.2	7.0	7.7	6.0	7.0

* HF=High Flow; MF = Mean Flow; LF = Low Flow

** Water was manually sampled every 5 min.

*** The outlet water was sampled every 2 hours until the bromide concentration was lower than the limit of quantification (50 µg/L)

**** Three water depths were measured inside the CWs: in the $1^{st}/2^{nd}/3^{rd}$ ponds and in the inlet/expansion/outlet of the ditch.

Table 3. Transport parameters derived from the Residence Time Distribution analysis for the pond and ditch under distinct flow rates

	t_n (h)	t_{mean} (h)	$t_\theta = e_v$	N	λ	t_{10}/t_n	t_{90}/t_{10}	Pe	v_{mean} (m/min)
Pond-HF	1.7	1.5	0.87	2.3	0.50	0.48	2.3	62	0.53
Pond-MF	2.5	2.2	0.89	2.5	0.53	0.46	2.1	1697	0.36
Pond-LF	37.2	23.0	0.62	1.4	0.18	0.14	10.7	11	0.03
Ditch-MF	2.5	0.8	0.32	1.3	0.07	0.20	1.7	28	1.55
Ditch-LF	13.0	1.4	0.11	1.1	0.01	0.07	2.1	16	0.87

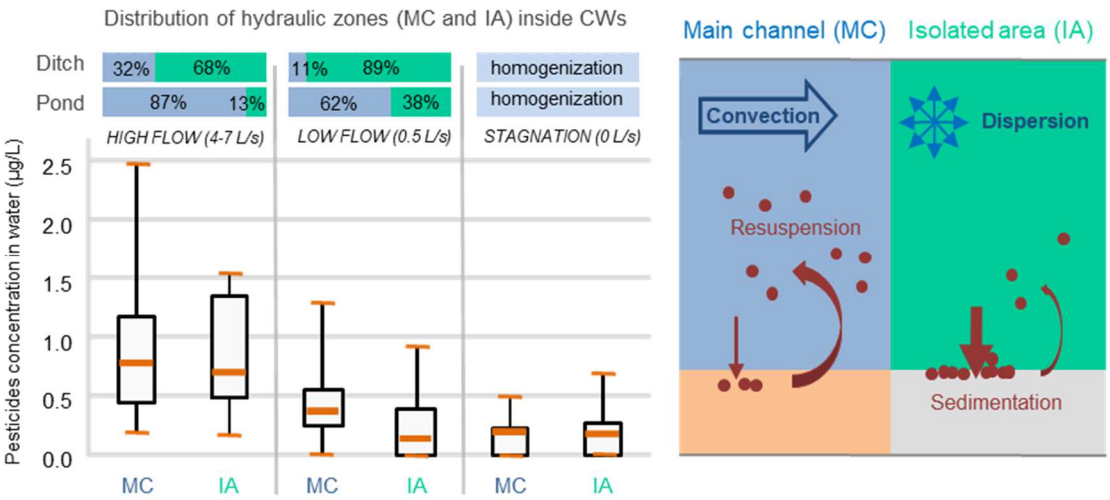
Distribution of hydraulic zones (MC and IA) inside CWs
Ditch
Pond
32%
68%
87%
13%
11%
89%
62%
38%
homogenization
homogenization
HIGH FLOW (4-7 L/s)
LOW FLOW (0.5 L/s)
STAGNATION (0 L/s)
Pesticides concentration in water (µg/L)
2.5
2.0
1.5
1.0
0.5
0.0
MC
IA
MC
IA
MC
IA
Main channel (MC)
Isolated area (IA)
Convection
Dispersion
Resuspension
Sedimentation